Cell Death and Differentiation (2006) 13, 1156–1169

www.nature.com/cdd

BCL-x_L: time-dependent dissociation between modulation of apoptosis and invasiveness in human malignant glioma cells

M Weiler[1], O Bähr[1], U Hohlweg[1], U Naumann[1], J Rieger[1], H Huang[2], G Tabatabai[1], HW Krell[3], H Ohgaki[2], M Weller[1] and W Wick*[,1]

[1] Laboratory of Molecular Neuro-Oncology, Department of General Neurology and Hertie Institute for Clinical Brain Research, University of Tübingen, Hoppe-Seyler-Str. 3, Tübingen D-72076, Germany
[2] Unit of Molecular Pathology, International Agency for Research on Cancer, 150 cours Albert Thomas, Lyon 69372, France
[3] Roche Diagnostics GmbH, Pharma Research Penzberg, Screening Technologies, Penzberg 82377, Germany
* Corresponding author: W Wick, Laboratory of Molecular Neuro-Oncology, Department of General Neurology and Hertie Institute for Clinical Brain Research, Hoppe-Seyler-Str. 3, Tübingen D-72076, Germany.
Tel: +49 7071 298 0461; Fax: +49 7071 29 5260;
E-mail: wolfgang.wick@uni-tuebingen.de

Received 21.2.05; revised 19.8.05; accepted 26.8.05; published online 28.10.05
Edited by G Nunez

Abstract

Conditionally BCL-x_L-overexpressing LNT-229 Tet-On glioma cell clones were generated to investigate whether the 'antiapoptosis phenotype' and the 'motility phenotype' mediated by BCL-2 family proteins in glioma cells could be separated. BCL-x_L induction led to an immediate and concentration-dependent protection of LNT-229 cells from apoptosis. BCL-x_L induction for up to 3 days did not result in altered invasiveness. In contrast, long-term BCL-x_L induction for 21 days resulted in increased transforming growth factor-β_2 expression, and in metalloproteinase-2 and -14 dependent, but integrin independent, increased invasiveness. Withdrawal of doxycycline (Dox) abolished the protection from apoptosis whereas the 'invasion phenotype' remained stable. Dox stimulation of BCL-x_L-inducible LNT-229 cells conferred infiltrative growth to BCL-x_L-positive glioma cells *in vivo* and reduced the survival of tumor-bearing mice. These data allow to dissect a direct antiapoptotic action of BCL-x_L from an indirect effect, presumably mediated by altered gene expression, which modifies tumor cell invasiveness *in vitro* and *in vivo*.

Cell Death and Differentiation (2006) **13,** 1156–1169.
doi:10.1038/sj.cdd.4401786; published online 28 October 2005

Keywords: anoikis; BCL-x; glioma; invasiveness; metalloproteinase; Tet-On system; TGF-β

Abbreviations: AnxV, Annexin V; (BCL)-2, B-cell leukemia/lymphoma-like protein; CD95L, cluster differentiation 95 ligand; CHX, cycloheximide; Dox, doxycycline; DMEM, Dulbecco's Modified Eagle's Medium; ERK, extracellular-related kinase; FCS, fetal calf serum; FITC, fluorescein isothiocyanate; HGF, hepatocyte growth factor; (c.4.2, c.10.1, and c34.2), LNT-229 Tet-On control; (c4.2E, c10.1D, c10.1J,and c34.2A), LNT-229 BCL-x_L Tet-On; MAPK, mitogen-activated protein kinase; MMP, matrix metalloproteinase; MT1-MMP/MMP-14, membrane-type 1-MMP; (NF)κB, nuclear factor; *o*-PA, ortho-phenantroline; PI, propidium iodide; rTetR, reverse Tet repressor; TRE, tet-responsive element; SN, supernatant; TGF, transforming growth factor

Introduction

Gliomas are paradigmatic for their propensity to deeply infiltrate adjacent brain tissue precluding definitive surgical resection and limiting the efficacy of other local therapies. The failure of traditional cancer therapies results, among others, from defects in the apoptotic machinery of glioma cells, accounting for their resistance to irradiation and chemotherapy. The balance of B-cell leukemia/lymphoma-like protein (BCL)-2 family proteins may confer constitutive and therapy-inducible resistance. The expression of antiapoptotic BCL-2 family proteins increases during the natural course of gliomas.[1] Additionally, their preferential localization at the outer mitochondrial membrane indicates that they maintain mitochondrial homeostasis upon withdrawal from growth factors.[2] However, a substantial fraction of antiapoptotic BCL-x_L has been found in a 50 kDa cytosolic homodimer complex in nontumor cells exogenously expressing BCL-x_L, addressing the question of additional cytosolic effects.[3] Other BCL-2 family proteins locate physiologically to intracellular membranes.[4] BCL-2 family proteins have mainly been studied as positive or negative regulators of apoptosis. However, one requirement for successful migration and invasion of glioma cells is their resistance to the endogenous death program of apoptosis once the cell has detached from the primary tumor tissue. Further, malignant progression correlates with increased migratory capacity involving a wide range of molecular mechanisms including metalloproteinolytic activity and integrin-dependent regulation of cell adhesion. Invasion of cells into the surrounding tissue is a multistep process which requires changes in cell–cell contacts, for example, mediated by cadherins or the hyaluronic acid receptor CD44,[5,6] cell–substrate interactions and degradation of the extracellular matrix by metalloproteinases (MMP). Some cytokines such as epidermal growth factor (EGF), hepatocyte growth factor (HGF) or transforming growth factor (TGF)-β_2 promote cell migration and invasion in a cell type- and context-dependent manner by triggering distinct intracellular signaling cascades.[7,8] Accordingly, expression of TGF-β_2 correlates with glioma cell invasiveness[9] and inhibition of TFG-β by a neutralizing antibody or by a small molecule TGF-β receptor

antagonist, SD-208, significantly reduced glioma cell migration.[10,11]

Ectopic expression of the antiapoptotic BCL-2 protein conferred a more migratory and invasive phenotype to two human malignant glioma cell lines *in vitro.*[12] The inter-relation between proteins of the BCL-2 family and motility has also been shown for other tumor types.[13] Further, the exogenous expression of BCL-2 in endothelial cells enhanced intratumoral angiogenesis and growth of experimental squamous cell carcinomas and Kaposi's sarcomas.[14] However, it remains unclear whether the promotion of migration and invasiveness is independent of the antiapoptotic properties of BCL-2. In a comprehensive analysis and correlation of key molecular and biologic prerequisites of glioma cell migration and invasion, an expression pattern of BCL-2 family proteins favoring resistance to apoptosis was associated with enhanced migration, invasion, TGF-β_2 mRNA and protein expression and activity, and MMP activity.[15]

In the present study, we aimed at dissociating the 'apoptosis phenotype' from the 'motility phenotype' of glioma cells and asked whether both phenotypes are modulated by different intracellular thresholds or kinetics of BCL-x_L expression or secondary effects of BCL-x_L overexpression.

Results

Concentration-dependent induction of BCL-x_L transgene expression *in vitro*

To investigate whether there is a specific propensity of BCL-2 family proteins to promote migration and invasiveness of glioma cells, we used a Tet-On gene expression system to generate several human LNT-229 glioma sublines permitting conditional expression of BCL-x_L under the control of a tet-responsive element (TRE) in the presence of doxycycline (Dox) and of a reverse Tet repressor (rTetR). Immunoblot analysis of a representative LNT-229 BCL-x_L Tet-On clone 34.2A (c34.2A) revealed an inducible BCL-x_L dependent on Dox concentrations ranging from 0.175 to 2.0 μg/ml relative to β-actin loading controls. c34.2 was chosen as a noninducible Tet-On vector control (Figure 1a). There was no difference in BCL-x_L expression after exposure to Dox for 3 and 21 days, respectively, at a concentration (2 μg/ml) sufficient to produce a maximum protein level of BCL-x_L at 3 days. The withdrawal from Dox during a subsequent period of another 5 days reset BCL-x_L expression to the level observed in unstimulated c34.2A cells (Figure 1b). The responsiveness to Dox depicted in Figure 1 is representative for each of the four BCL-x_L Tet-On clones (designated as c4.2E, c10.1D, c10.1J, and c34.2A) used in the further experiments (data not shown).

No translocation of exogenous BCL-x_L from the mitochondria

Sequestration of BCL-x_L to the cytosol[2] and the association of BCL family proteins with migration and invasion suggested that exogenously expressed BCL-x_L might translocate to cellular compartments other than the mitochondria, for example the inner cell membrane in glioma cells. We

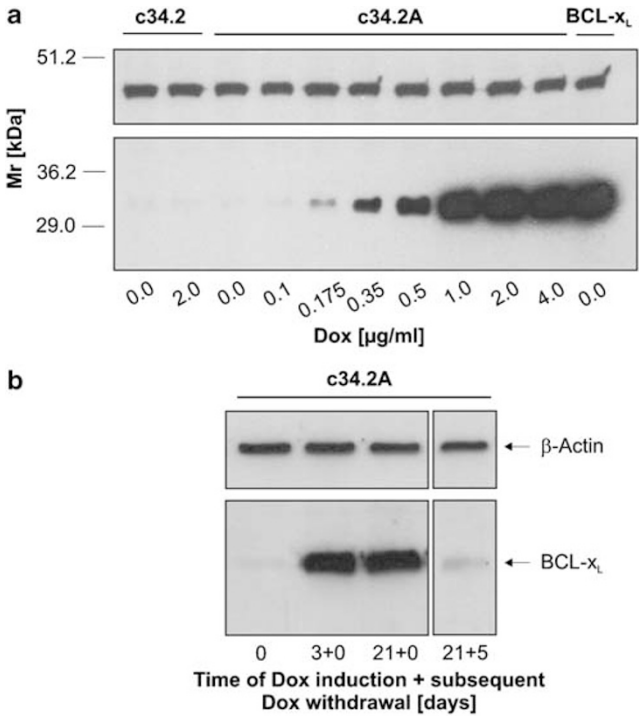

Figure 1 Stably transfected human LNT-229 BCL-x_L Tet-On glioma cell clones display Dox-dependent induction of BCL-x_L protein expression. (**a**) BCL-x_L protein levels in whole cell lysates of c34.2 and c34.2A glioma cells at 72 h exposure to Dox were examined by immunoblot analysis using a monoclonal anti-human BCL-x antibody. The BCL-x_L expression level of a constitutive LNT-229 BCL-x_L glioma transfectant (referred to as BCL-x_L) was included as a positive control in the right lane. (**b**) The same antibody was used to examine BCL-x_L expression in naïve cells (lane 1) and after 72 h of incubation with Dox at 2 μg/ml (lane 2) compared with long-term incubation of 21 days, with (lane 4) or without (lane 3) a subsequent withdrawal from Dox for another 5 days

therefore assessed the subcellular localization of BCL-x_L in LNT-229 BCL-x_L Tet-On cells using confocal laser scanning microscopy. Figure 2 demonstrates a strong induction of BCL-x_L-specific mitochondrial immunofluorescence after exposure to Dox for 3 (Figure 2e) and 21 days (Figure 2h) compared with Dox-treated c34.2 control cells (Figure 2j and k).

Induction of BCL-x_L inhibits apoptosis in a concentration-dependent manner

The next set of experiments assessed the antiapoptotic function of inducible BCL-x_L. We observed an inducible BCL-x_L-dependent protection from staurosporine-induced apoptosis as assessed by flow cytometry using annexin V (AnxV)-fluorescein isothiocyanate (FITC) staining, a technique that measures the exposure of phosphatidylserine on the cell membrane at early stages of apoptosis and propidium iodide (PI) staining, a technique to measure loss of membrane integrity (Figure 3a). There was no difference in staurosporine sensitivity between 3 and 28 days of BCL-x_L induction. Withdrawal from Dox for 3 days or longer abolished the antiapoptotic effect (Figure 3b). Second, in order to corroborate the inducible BCL-x_L-mediated antiapoptotic properties in an independent paradigm, we performed crystal violet

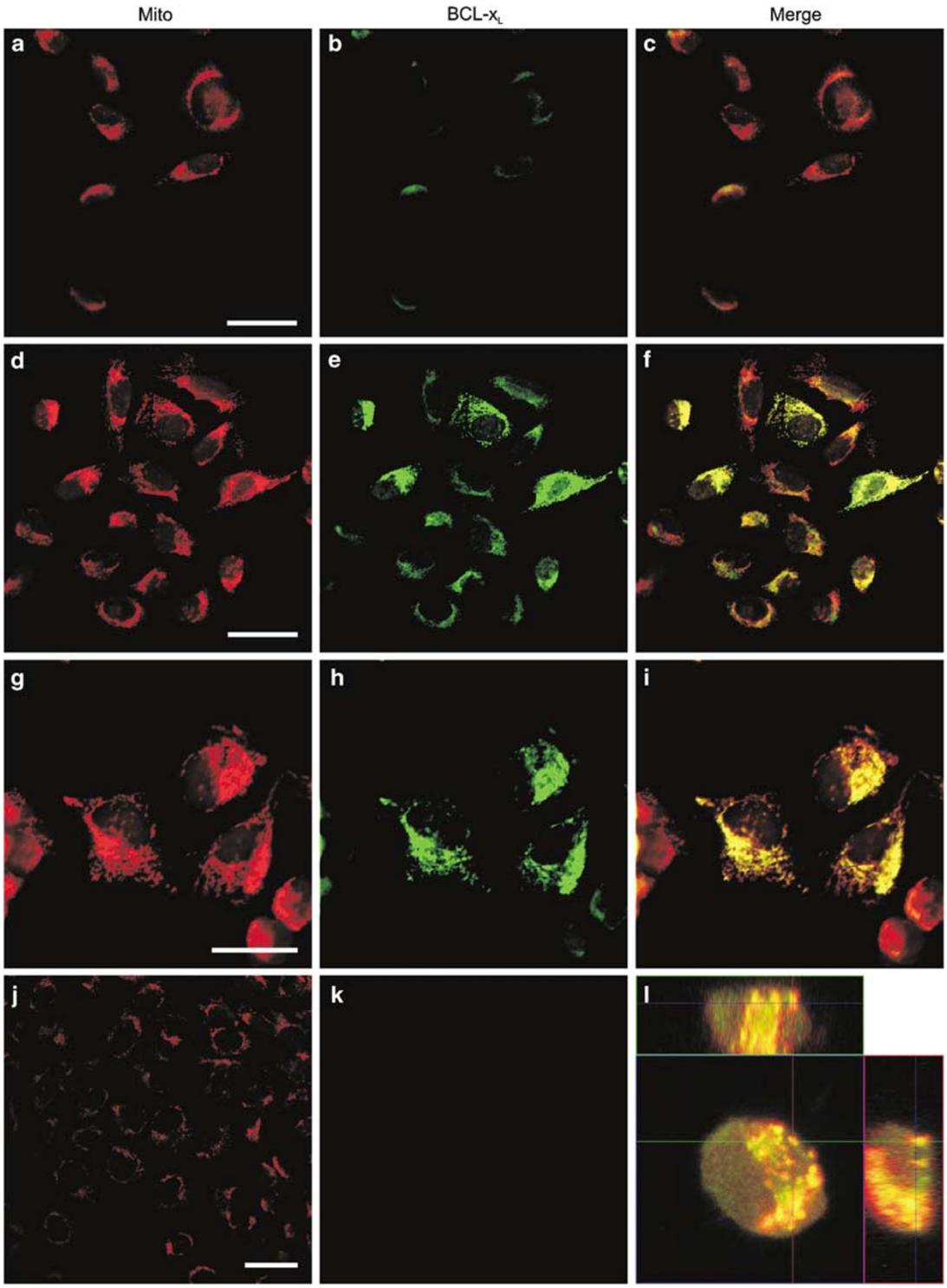

Figure 2 BCL-x_L-specific mitochondrial immunofluorescence is conditionally inducible in c34.2A cells and does not display subcellular translocation following long-term induction. c34.2A glioma cells, untreated (**a**–**c**) or exposed to Dox (2 μg/ml) for 3 days (**d**–**f**) or 21 days (**g**–**i** and **l**), or c34.2 control cells, untreated or pretreated with Dox for 3 days (**j** and **k**) were incubated with red-fluorescent MitoTracker, immuno-labeled using anti-BCL-x and green-fluorescent secondary antibodies, and analyzed by confocal laser scanning microscopy using appropriate filters for visualization of red (**a**, **d**, **g** and **j**), green (**b**, **e**, **h** and **k**), or combined (**c**, **f**, **i** and **l**) fluorescence. (**l**) BCL-x_L-specific immunofluorescence (green) and mitochondrial fluorescence (red) colocalize (yellow) in a three-dimensional confocal image of a c34.2A cell following BCL-x_L long-term induction of 21 days (scale bars, 10 μm)

staining-based cell viability assays using the death ligand cluster differentiation 95 ligand (CD95L) (Figure 3c and d) and the two chemotherapeutics, lomustine and doxorubicin (data not shown), as apoptosis-inducing agents. The induction of BCL-x_L enhanced viable cell counts in a concentration-dependent manner in cells exposed to CD95L (Figure 3c).

Similar to the results obtained in the AnxV-FITC and PI stainings, we observed no difference in protection from CD95L-induced apoptosis conferred by BCL-x_L induction for 28 days compared with 3 days, and withdrawal from Dox for 3 days or more abolished the antiapoptotic effect (Figure 3d). As expected, apoptosis in control cells was prevented by preincubation with zVAD-fmk, an irreversible broad-spectrum caspase inhibitor (data not shown).

Long-term induction of BCL-x_L is required to enhance glioma cell invasion

We next examined the invasive phenotype of c10.1 and c10.1J cells *in vitro*. Surprisingly, at Dox concentrations sufficient to produce maximum protection against apoptosis (2 μg/ml; Figure 3a and c), we observed no difference between the number of invading untreated c10.1J cells and invading c10.1J cells following a BCL-x_L induction of 3 days. Constitutively BCL-x_L-overexpressing cells served as a positive control in this experiment. The Dox concentrations applied here had no intrinsic effect on invasion. We assayed the glioma cell phenotype following periods of Dox induction of 7, 10, 14 and 21 days in *trans*-membrane invasion and spheroid invasion into a collagen I matrix. Conditional expression of BCL-x_L for 21 days resulted in a five-fold increase in invasiveness that remained stable after a 5 days withdrawal from Dox and was even still significantly enhanced after 21 days of withdrawal. Importantly, inhibition of MMP using ortho-phenantroline (*o*-PA) (data not shown) or the specific MMP inhibitor RO-28-2653[17] blocked BCL-x_L-in-

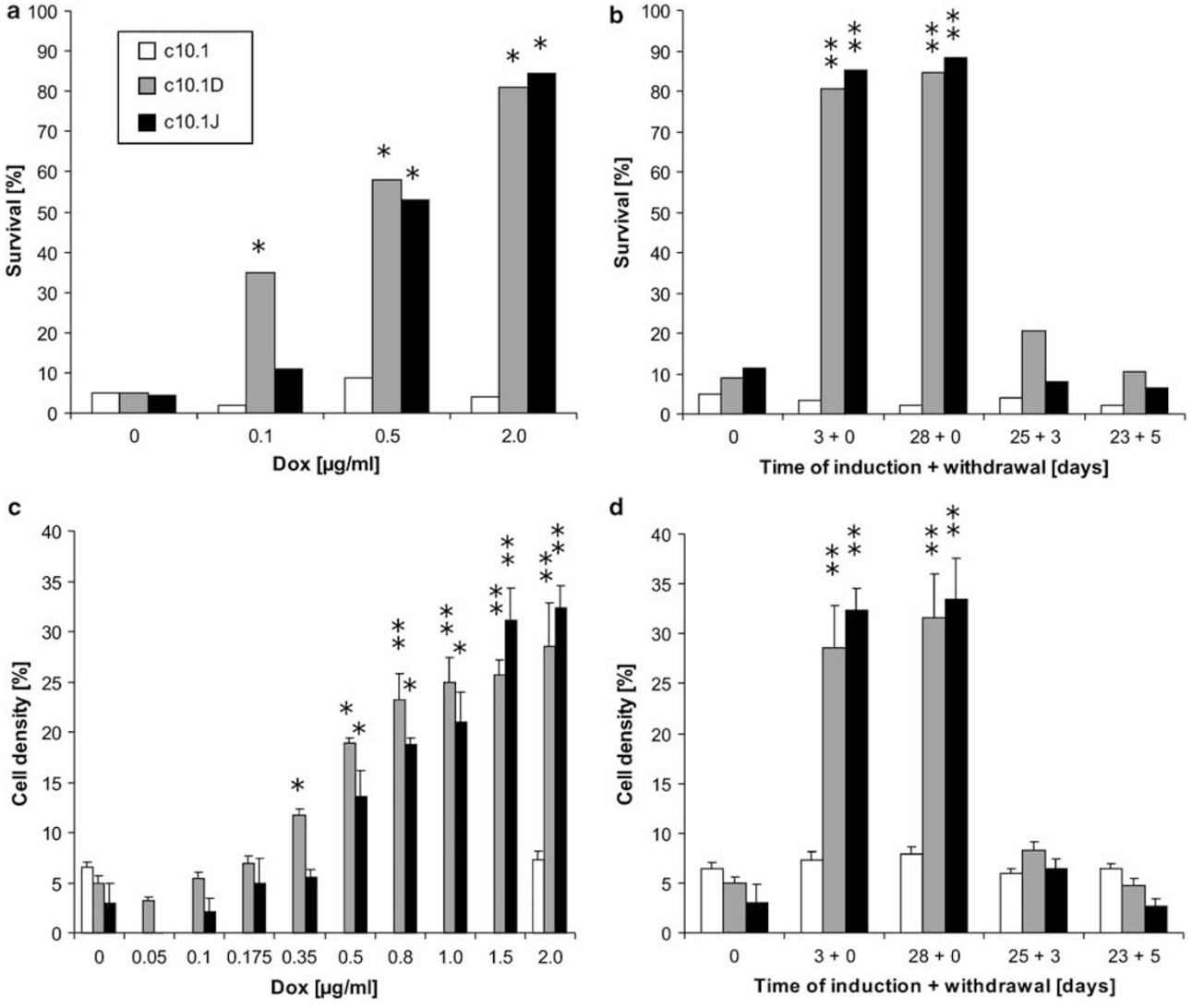

Figure 3 BCL-x_L concentration-dependent resistance of malignant glioma cells towards apoptosis. (**a**) c10.1 control, c10.1D or c10.1J glioma cells exposed to Dox for 72 h were treated with staurosporine at 20 μM for 6 h and subsequently analyzed for AnxV-FITC/PI staining by flow cytometry. (**b**) Naïve cells and cells exposed to Dox for 3 or 28 days, with or without a subsequent withdrawal from Dox for another 3 or 5 days, were treated with staurosporine for 6 h and analyzed as in (**a**). Data in (**a** and **b**) are expressed as mean percentages of AnxV- and PI-negative (surviving) cells ($n=3$) (*$P<0.05$ and **$P<0.01$ compared with c10.1 cells). (**c**) Cells exposed to Dox for 72 h were treated with CD95L (120 U/ml) and CHX (10 μg/ml) for 6 h and viable cell counts were assessed by crystal violet staining. (**d**) Cells pretreated with Dox as in (**b**) as indicated and subsequently incubated with CD95L and CHX as in (**c**) were stained with crystal violet. Data are expressed as mean optical densities and S.E.M. ($n=3$) (*$P<0.05$ and **$P<0.01$ compared with c10.1 cells)

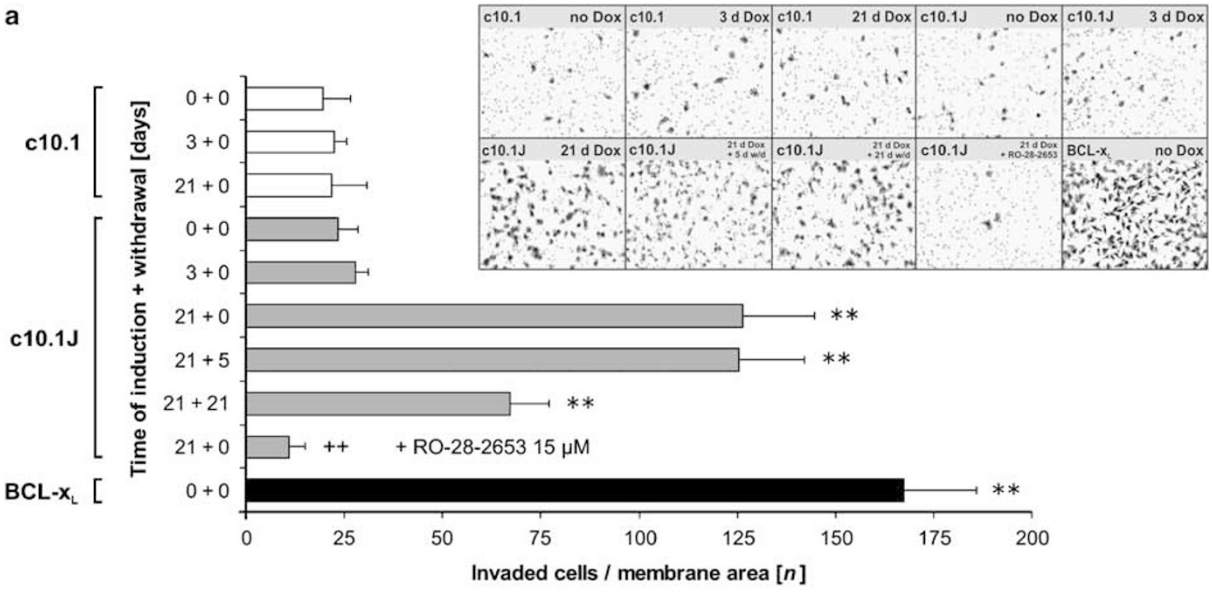
a
c10.1 no Dox
c10.1 3 d Dox
c10.1 21 d Dox
c10.1J no Dox
c10.1J 3 d Dox
c10.1J 21 d Dox
c10.1J 21 d Dox + 5 d w/d
c10.1J 21 d Dox + 21 d w/d
c10.1J 21 d Dox + RO-28-2653
BCL-xL no Dox
c10.1
c10.1J
BCL-xL
Time of induction + withdrawal [days]
0 + 0
3 + 0
21 + 0
0 + 0
3 + 0
21 + 0
21 + 5
21 + 21
21 + 0
0 + 0
++
+ RO-28-2653 15 µM
**
**
**
**
0
25
50
75
100
125
150
175
200
Invaded cells / membrane area [n]

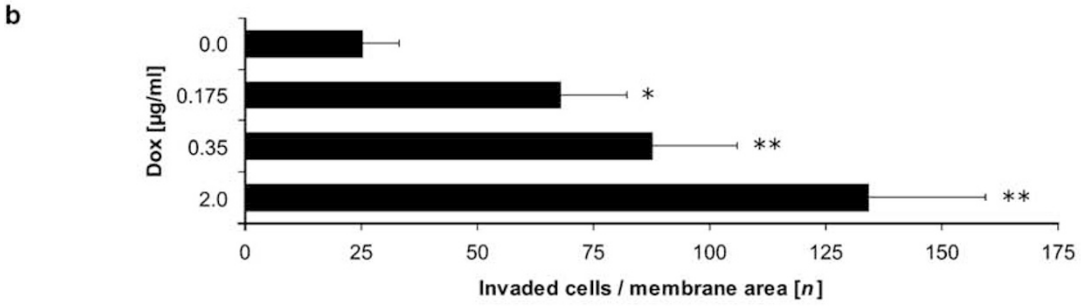
b
Dox [µg/ml]
0.0
0.175
0.35
2.0
*
**
**
0
25
50
75
100
125
150
175
Invaded cells / membrane area [n]

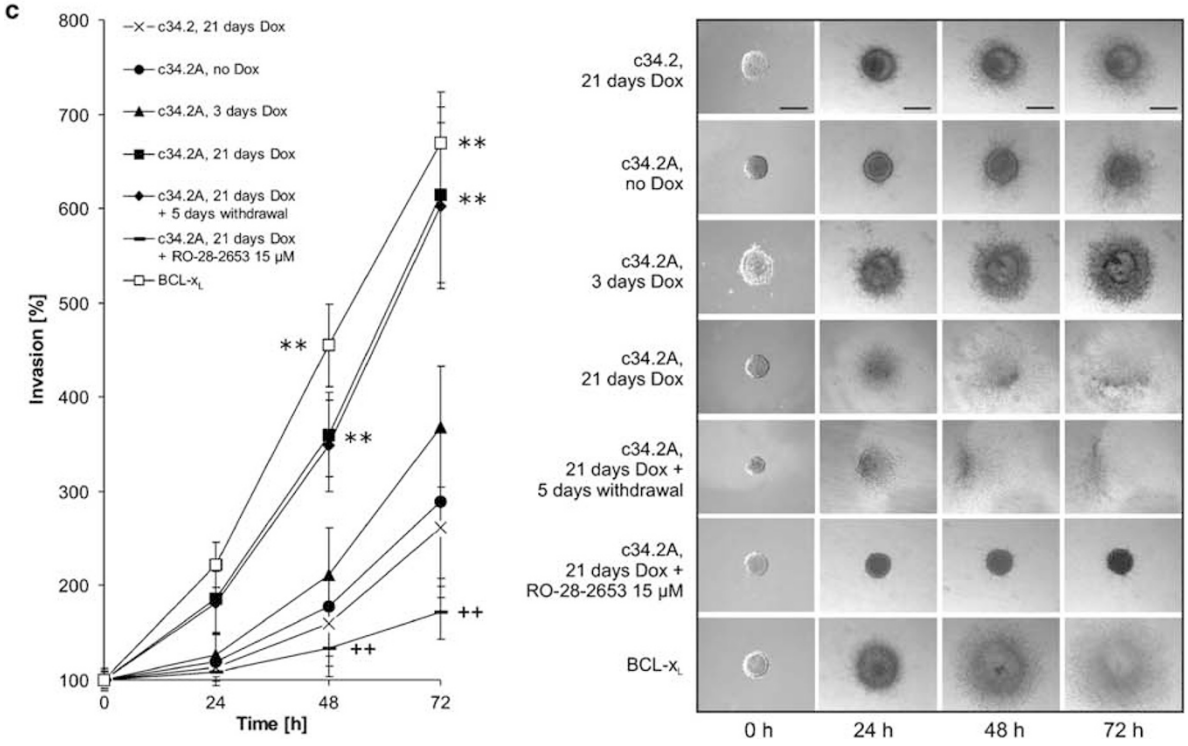
c
c34.2, 21 days Dox
c34.2A, no Dox
c34.2A, 3 days Dox
c34.2A, 21 days Dox
c34.2A, 21 days Dox + 5 days withdrawal
c34.2A, 21 days Dox + RO-28-2653 15 µM
BCL-xL
Invasion [%]
800
700
600
500
400
300
200
100
**
**
**
++
++
0
24
48
72
Time [h]
c34.2, 21 days Dox
c34.2A, no Dox
c34.2A, 3 days Dox
c34.2A, 21 days Dox
c34.2A, 21 days Dox + 5 days withdrawal
c34.2A, 21 days Dox + RO-28-2653 15 µM
BCL-xL
0 h
24 h
48 h
72 h

duced invasiveness below baseline levels (Figure 4a), corroborating an essential role for MMP in BCL-x_L-mediated invasiveness. In contrast, exposure to zVAD-fmk for 21 days did not alter the invasive phenotype of c10.1 and c10.1J cells (data not shown). Figure 4b demonstrates that the induction of invasiveness is dependent from BCL-x_L concentrations. Even a slight induction of BCL-x_L expression achieved at a Dox concentration of 0.175 μg/ml over 21 days led to a pronounced stimulation of invasiveness. We also examined the invasion of multicellular glioma spheroids of c34.2 and c34.2A cells in three-dimensional collagen I gel matrices enriched with fibronectin. Consistent with the results obtained in the matrigel invasion assays, only long-term induction of BCL-x_L for 21 days but not for 3 days led to enhanced cell invasion into collagen gel matrices, which was maintained after a withdrawal from Dox (Figure 4c). These results were confirmed for all other independently generated BCL-x_L Tet-On clones (c4.2E, c10.1D, c10.1J and c34.2A). Next we analyzed whether alterations in the expression or activity of integrin heterodimers mediated the delayed BCL-x_L-dependent promotion of invasiveness. Integrins are critically involved in radiation-induced stimulation of migration and invasiveness and are important for cell death induced by detachment from the basal lamina (*anoikis*).[15,16] However, flow cytometry using antibodies towards $\alpha_5\beta_1$- or $\alpha_v\beta_3$-integrin heterodimers as well as to the activated β_1 chain failed to reveal significant differences between BCL-x_L-expressing and control cells (data not shown). Further, analyzing spheroid invasion into matrices composed of different extracellular matrix proteins (collagen IV, fibronectin, laminin, vitronectin) did not demonstrate preferential utilization of any substrate by c34.2 or c34.2A cells at different Dox incubation intervals (data not shown). The detachment of c34.2A cells expressing BCL-x_L for 3 and 21 days, respectively, or of c34.2 control cells applying RGD peptides for 24 and 48 h resulted in similar fractions of apoptotic cells, and the same number of colonies could be grown from either subclone (data not shown).

Enhanced clonogenicity, but lack of metabolic differences in the BCL-x_L-expressing clones

Induction of BCL-x_L for 3 days or longer increased colony formation in clonogenicity assays. This effect was sensitive to withdrawal from Dox (Figure 5a). In contrast, there were no significant differences in proliferation determined by [methyl-^{3}H]-thymidine-incorporation under normal or serum-free culture conditions (Figure 5b). Further, glucose concentration (Figure 5c), ATP levels and pH (data not shown) remained stable in cells that had been induced with Dox for 3 or 21 days.

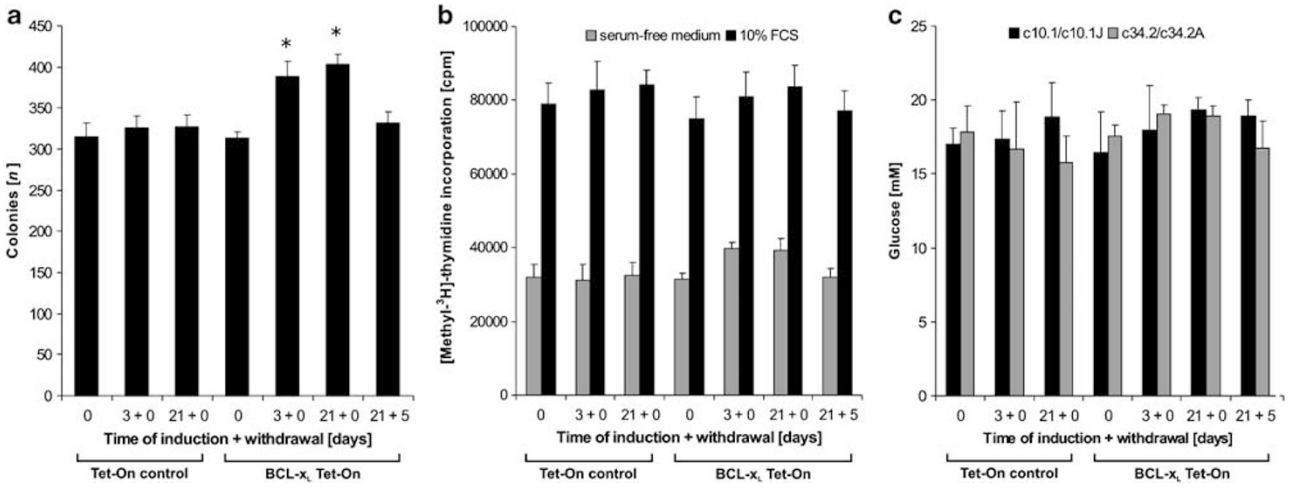

Figure 5 Short- and long-term induction of BCL-x_L enhances clonogenicity, but does not modulate proliferation or glucose metabolism of malignant glioma cells. LNT-229 Tet-On control (c10.1 and c34.2) or BCL-x_L-inducible (c10.1J and c34.2A) cells were treated with Dox (2 μg/ml) for 3 or 21 days, with or without a subsequent withdrawal from Dox for another 5 days and assessed for colony formation (**a**), [methyl-^{3}H]-thymidine incorporation (**b**) and glucose levels (**c**). Data are expressed as mean and SEM ($n=3$, $^*P<0.05$)

Figure 4 Long-term induction of BCL-x_L expression promotes invasiveness of human malignant glioma cells *in vitro*. (**a**) c10.1 or c10.1J glioma cells, naïve or preincubated with Dox (2 μg/ml) for 3 or 21 days, with or without a subsequent withdrawal from Dox for further 5 or 21 days and with or without exposure to RO-28-2653, were analyzed for invasiveness in matrigel invasion chambers. A constitutively BCL-x_L overexpressing LNT-229 transfectant (referred to as BCL-x_L) was included (see also Figure 1a). Invading cells were counted in five random fields (mean and S.E.M., $n=3$, $^{**}P<0.01$ relative to c10.1). Representative filters demonstrating BCL-x_L-dependent stimulation of glioma cell invasion are depicted in the upper right panel (at magnification $\times$ 100, inset). (**b**) c10.1J glioma cells preincubated with Dox at indicated concentrations for 21 days were analyzed as in (**a**). (**c**) c34.2 and c34.2A glioma cells, pretreated as indicated, and the constitutive BCL-x_L transfectant were analyzed for invasion from preformed spheroids into a protein gel matrix consisting of collagen I enriched with fibronectin. The radial distance from the center of each spheroid was measured for 30 representative migrated cells in intervals of 24 h. Data are expressed as percentages of the mean migrated distance relative to the initial radius of each individual spheroid at 0 h (mean and S.E.M., $n=3$, $^{**}P<0.01$ relative to c34.2; left panel). Representative glioma spheroids at each time are depicted (scale bars, 400 μm; right panel)

Long-term expression of BCL-x_L promotes TGF-β_2 and MMP-2 expression

To elucidate the molecular mechanisms underlying the increased invasiveness mediated by long-term induction of BCL-x_L, we performed cDNA arrays (Cancer 1.2 and apoptosis arrays) of c10.1J cells treated with Dox for 3 and 21 days. c10.1 cells treated with Dox for 21 days served as controls in this analysis. Interestingly, mRNA specific for TGF-β_2 (4.5-fold), MMP-2 (2.2-fold) and MT1-MMP (2.5-fold) were upregulated while tissue inhibitor of MMP (TIMP)-2 (0.6-fold) was downregulated in c10.1J cells exclusively following long-term exposure to Dox relative to Dox-treated c10.1 control cells. These data were confirmed by TGF-β_2-specific immunoblot analyses (Figure 6a). Importantly, we observed only an insignificant increase in the 55 kDa proform of the TGF-β_2 protein while expression of the 12.5 kDa form of the mature TGF-β_2 protein was significantly induced only after long-term treatment with or without subsequent downregulation of BCL-x_L. Yet, baseline expression levels of TGF-β_2 in untreated c34.2A cells were lower than in c34.2 controls (Figure 6a). This observation is relevant with respect to the resulting invasive phenotype since application of a neutralizing TGF-β antibody abolished the proinvasive effect in long-term BCL-x_L-induced c10.1J cells (Figure 6b). Recent data place TGF-β_2 upstream of MMPs in the motile phenotype of glioma cells.[9]

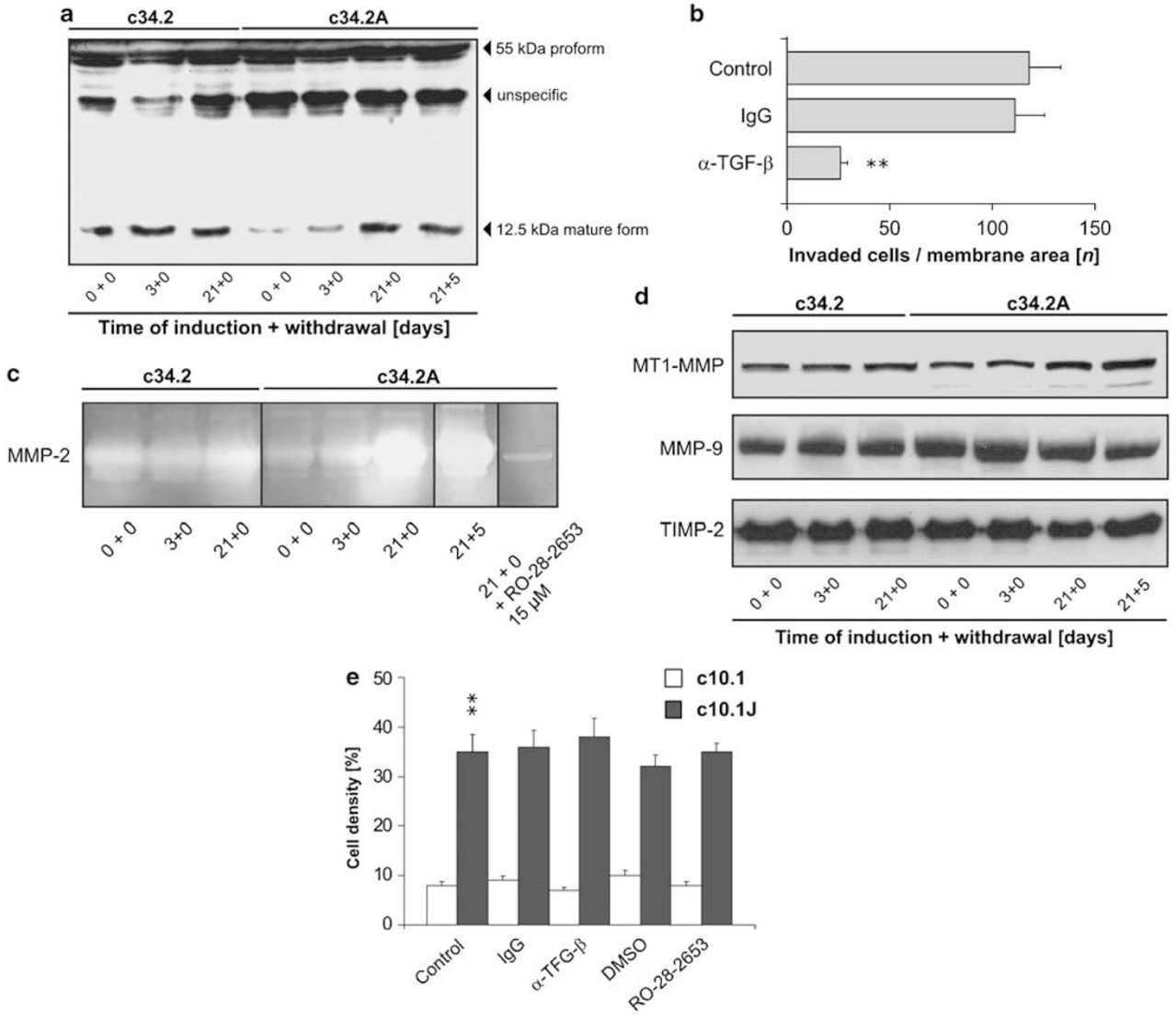

Figure 6 BCL-x_L-mediated invasiveness depends on enhanced TGF-β_2 expression and MMP-2 activity. (**a**) TGF-β_2 protein expression was examined by immunoblot. (**b**) c10.1J glioma cells, preincubated with Dox (2 μg/ml) for 21 days and neutralizing TGF-β_2 or control antibodies (2 μg/ml) for 24 h, were analyzed for invasiveness in matrigel invasion chambers. Invading cells were counted in five random fields (mean and S.E.M., $n=3$, $^{**}P<0.01$ for the effect of α-TGF-β_2). (**c**) c34.2 control or BCL-x_L-inducible c34.2A cells were incubated with Dox (2 μg/ml) for 3 or 21 days with or without a subsequent withdrawal from Dox for another 5 days or in the presence of RO-28-2653 for 24 h. MMP-2 activity in serum-free SN was assessed by gelatin zymography. (**d**) Expression levels of MT1-MMP in whole cell lysates and of MMP-9 and TIMP-2 in SN were examined by immunoblot. Experiments were repeated at least three times with similar results. Representative data are depicted. (**e**) Cells exposed to Dox for 72 h and either coincubated with standard culture medium, control IgG, α-TGF-β_2, DMSO or RO-28-2653 for further 24 h were treated with CD95L (120 U/ml) and CHX (10 μg/ml) for 6 h. Viable cell counts were assessed and data are expressed as in Figure 3d (mean and S.E.M., $n=3$)

Table 1 Long-term expression of BCL-x_L induces MMP-2 activity and expression of TGF-β_2 and MT1-MMP

	3 days		21 days		21+5 days
	c34.2	**c34.2A**	**c34.2**	**c34.2A**	**c34.2A**
Furin	0.93	1.05	0.91	0.96	1.03
pMAPK/pERK	1.08	0.5	1.08	0.42	0.41
MMP-2	0.99	1.01	1.02	1.1	1.03
MMP-2 activity	0.98	1.07	1.1	**5.42**	**5.32**
MMP-9	1.05	1.32	1.07	1.05	0.99
MMP-9 activity	1.13	1.21	1.14	1.29	1.26
MT1-MMP	1	0.97	1.1	**1.71**	**1.74**
NF-κB	1.16	1.02	1.18	1.03	0.99
TGF-β_1	1.09	1.05	1.11	0.92	1.01
TGF-β_2	1.1	1.21	1.1	**2.88**	**2.78**
TIMP-2	1.02	1.08	1.03	0.91	1.07

Immunoblots or zymographies (for MMP-2 and -9) of c34.2 or c34.2A glioma cells treated as indicated were quantified by densitometry. A significant induction relative to day 0 is indicated by bold font ($n=3$; $P<0.05$, *t*-test, S.D. $<10\%$)

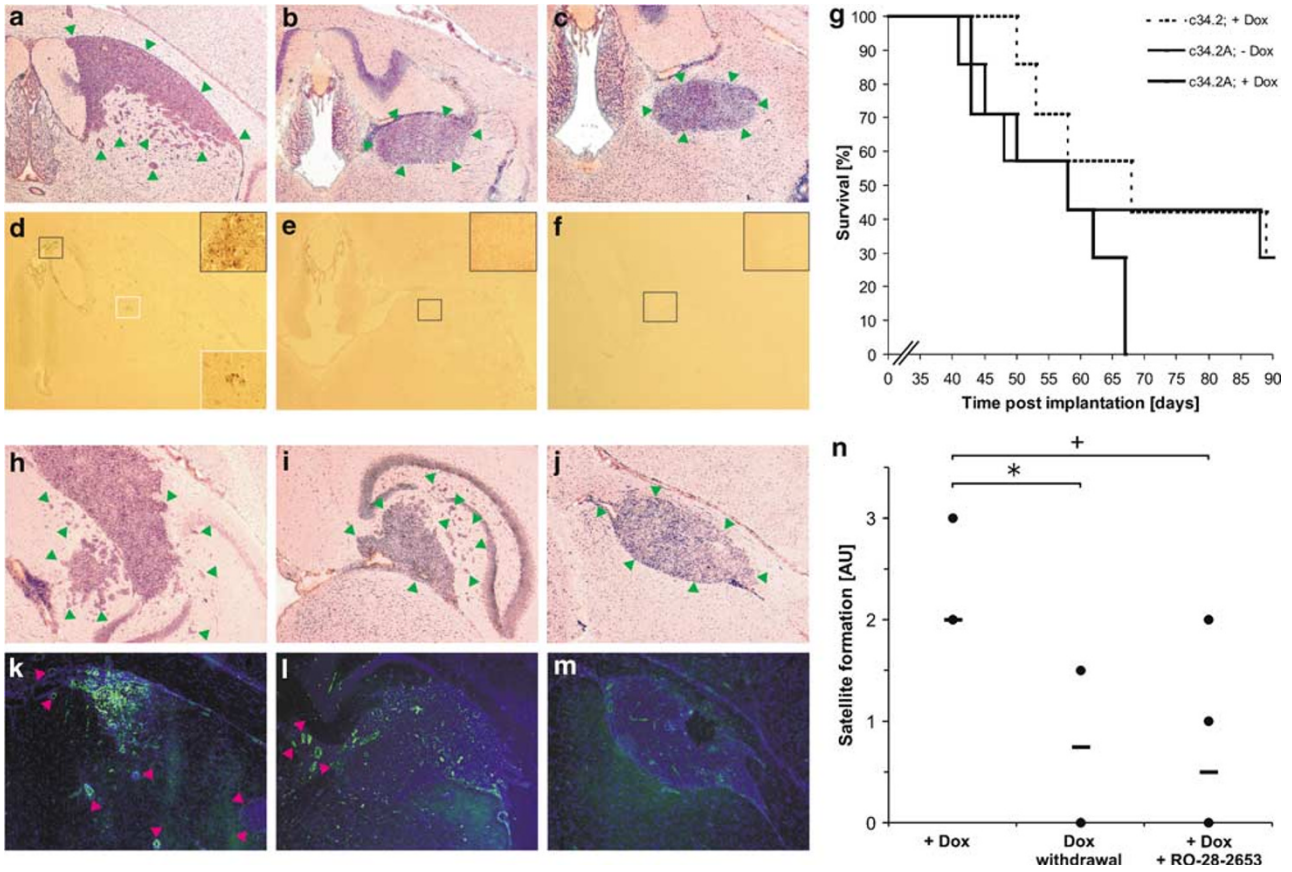

Figure 7 Induction of BCL-x_L expression promotes MMP-2-mediated invasiveness of xenografted human c34.2A glioma cells in brains of athymic mice and results in decreased survival. (**a–g**) Three groups of animals (each $n=9$) were formed: Dox (2 mg/ml) dissolved in 1% sucrose solution was applied as drinking water of mice that had been either implanted BCL-x_L-inducible c34.2A (group 1; **a**, **d** and **f**) or c34.2 control cells (group 2; **c**). As an additional control group, mice bearing c34.2A cells received sucrose solution only (group 3; **b** and **e**). Mice ($n=2$) of each group were killed on day 28. Brains were fixed, cut and either stained with hematoxylin–eosin (**a–c**) or immuno-labeled using a polyclonal anti-human BCL-x antibody (**d** and **e**) or an unspecific IgG control antibody (**f**). Depicted are transversal brain sections (8 μm) at magnification $\times 25$. Higher resolutions of immuno-stained tumor areas are inserted in small rectangles (magnification $\times 200$) (**d–f**). Solid tumor masses (**a–c**) and singular spread glioma cell satellites (**a**) are marked by green arrow heads. (**g**) In the same experimental setting, the remaining seven animals in each group were observed in daily intervals and killed at the onset of neurological symptoms. (**h–n**) BCL-x_L-inducible c34.2A cells that had been challenged with Dox *in vitro* for 21 days were subsequently implanted intracerebrally. Three groups of animals were formed: Dox application (2 mg/ml) was continued via the drinking water in the absence (group 1; $n=4$, **h** and **k**) or presence of RO-28-2653 (group 2, $n=6$; **j** and **m**) In the third animal group, Dox application was discontinued *in vivo* by applying sucrose solution only (group 3, $n=4$; **i** and **l**). For the assessment of tumor growth, all animals were killed on day 28 after tumor cell implantation. Cryostat transverse brain sections (8 μm) were stained with hematoxylin–eosin (**h–j**), and tumor-containing sections of each brain were used for *in situ* zymographies (**k–m**). Solid tumor masses (**h–j**) and singular spread glioma cell satellites (**h**, **i**, **k** and **l**) are marked by green (**h–j**) or pink (**k** and **l**) arrow heads. (**n**) Glioma satellite formation was quantified ($^*P<0.05$ for the effect of *in vivo* withdrawal from Dox and $^+P<0.05$ for the effect of RO-28-2653)

Quantitative RT-PCR for MMP-2 revealed an 1.8-fold increase of MMP-2 mRNA in LNT-229 c10.1J cells selectively after long-term induction of 21 days. Accordingly, MMP-2 expression and activity were markedly increased after long-term induction of BCL-x_L (Figure 6c). However, protein expression levels neither of MT1-MMP, MMP-9 nor of TIMP-2 were turned out to be regulated to a relevant extent (Figure 6d). An overall quantitative analysis of our immunoblots and zymographies is given in Table 1. AnxV-FITC/PI flow cytometry or crystal violet staining revealed no cytotoxicity of *o*-PA at 5 μM or RO-28-2653 at 15 μM, within the time frame of these experiments (data not shown). In contrast to the effects on invasiveness, inhibition neither of TGF-β nor of MMP attenuated the toxicity of CD95L/cycloheximide (CHX) in control or BCL-x_L-inducible cells (Figure 6e).

BCL-x_L expression confers infiltrative growth to LNT-229 tumors and reduces survival of tumor-bearing mice

We finally investigated the role of altered BCL-x_L expression in an intracerebral xenograft model in nude mice. The intracerebral implantation of unchallenged c34.2A cells and continuous *in vivo* induction of BCL-x_L via Dox-containing sucrose solution offered as drinking water resulted in highly invasive tumor growth as documented by the formation of tumor satellites not seen with Dox-treated c34.2 control cells or c34.2A cells grown in the brains of animals that received pure sucrose solution (Figure 7a–c). Consistently, we verified BCL-x_L transgene expression within both the tumor bulk and spread tumor satellites of Dox-induced c34.2A cells, but not in controls (Figure 7d–f). However, the volume of the main tumor mass did not significantly differ among the groups (data not shown). Yet, animals bearing BCL-x_L-induced tumors died earlier than controls (Figure 7g). Next, we implanted c34.2A cells that had been pretreated with Dox *in vitro* over 21 days and examined whether their invasive phenotype remained stable upon discontinuation of Dox exposure *in vivo*. Figure 7i and n illustrate that there was reduced satellite formation compared with tumors that were continued to be exposed to Dox *in vivo*. However, compared with noninvasively growing control tumors (as seen in Figure 7b and c), we observed still marked satellite formation and hence invasive growth accompanied by gelatinolytic activity within both the tumor bulk and singular satellites. Further, we confirmed that MMP inhibition by oral gavage of RO-28-2653 was effective even *in vivo*. Compared with Dox-induced but MMP-uninhibited tumors that showed massive MMP activity (Figure 7h and k), treatment with RO-28-2653 for 3 weeks prevented tumor satellite formation significantly (Figure 7j and n). The specificity of this treatment was corroborated by a dramatic loss of gelatinolytic activity in RO-28-2653-treated tumors (Figure 7k–m).

Discussion

The attribution to BCL-2 family proteins of functions other than regulation of apoptosis has remained controversial. Here we propose a novel proinvasive function of BCL-x_L separate from its antiapoptotic activity and illustrate how altered BCL-x_L expression confers an invasive phenotype *in vivo*. In generating conditionally BCL-x_L-expressing LNT-229 glioma cell clones, we aimed at elucidating whether the enhanced migration and invasiveness observed in stably BCL-2-transfected LNT-229 cells[12] was a selection effect or due to long-term culturing. We wanted to differentiate between the antiapoptosis phenotype and the motility phenotype on the basis of BCL-2 family protein expression levels.

Migration and invasion are prerequisites for the neoplastic phenotype of malignant gliomas, and malignant progression is correlated with increased migratory and invasive capacity. Previously, we defined a motility pathway for malignant glioma cells that included an interaction between HGF, the membrane–cytoskeleton linker ezrin, BCL-2 and TGF-β_2. In this paradigm, expression of a dominant-negative ezrin resulted in reduced BCL-2 expression levels and significantly reduced migration and invasiveness. However, the sensitivity towards chemotherapeutics, death ligands or therapeutic irradiation remained unaltered.[10] Since reduction of BCL-2 expression using antisense oligonucleotides strongly reduced survival of LNT-229 cells (data not shown) and since BCL-x_L is more relevant in human gliomas, we chose the alternative approach of generating conditionally BCL-x_L-overexpressing cells (Figures 1 and 2). We postulated that subtle changes in the expression level of BCL-2 family proteins would affect motility, but might not be sufficient to alter resistance towards apoptosis. Surprisingly, the opposite was the case (Figures 3 and 4): we observed a BCL-x_L concentration-dependent increase in resistance to different apoptotic stimuli up to Dox concentrations of 2 μg/ml whereas BCL-x_L expression at any level failed to influence the invasive phenotype of several LNT-229 BCL-x_L Tet-On subclones (c4.2E, c10.1D, c10.1J, and c34.2A) within the time frame of these experiments. Confirmation of these findings in several independently generated clones excluded spontaneous alterations in the long-term Dox-exposed cells to be causative for the invasive phenotype.

We next asked whether the induction of a motile phenotype conferred by BCL-x_L was a gradual, time-dependent effect, mimicking a paradigm for malignant progression. A highly significant induction of invasiveness in trans-membrane invasion and spheroid invasion into a collagen I/fibronectin matrix was found with induction of BCL-x_L for 21 days (Figure 4). Importantly, in contrast to the effects on resistance towards apoptosis, the pro-invasive phenotype conferred by long-term expression of BCL-x_L remained stable after withdrawal from Dox, that is, when BCL-x_L levels had returned to normal (Figures 3 and 4). To exclude that other measures of inhibiting apoptosis had the same impact on invasiveness like BCL-x_L, we analyzed long-term exposure (21 days) of c4.2E, c10.1D, c10.1J, and c34.2A cells to zVAD-fmk and did not observe any alterations in invasiveness (data not shown).

There is shedding of BCL-x_L homodimers into the cytosol.[3] Moreover, a Raf-1-binding site within the BH4 domain of BCL-2 might integrate pathways of resistance towards apoptosis with other cellular-signaling events.[18–20] It was therefore tempting to speculate that overexpression of BCL-x_L might result in a translocation of BCL-x_L to intracellular structures other than the mitochondria, for example the cytoskeleton or the inner cell membrane. However, confocal microscopy

demonstrated that this was not the case (Figure 2). Neither was there a translocation to the nuclear compartment.

Since radiation-induced glioma cell migration and invasion are inhibited by $\alpha_V\beta_3$-integrin antagonism[15] we assessed whether overexpression of BCL-x_L altered the sensitivity of glioma cells to membrane detachment-induced apoptosis. RGD peptide binding to integrins results in detachment-induced apoptosis in several cell types.[15,21,22] BCL-2 family proteins have been related to regulation of cell–cell contacts. However, the detachment of control cells or of c34.2A cells expressing BCL-x_L for 3 or 21 days using RGD peptides resulted in similar rates of apoptosis, indicating that overexpression of BCL-x_L did not protect from *anoikis*. Accordingly, flow cytometry for the activated β-integrin chain and expression of $\alpha_5\beta_1$- or $\alpha_v\beta_3$-integrin expression were unaltered by long-term BCL-x_L expression and invasion of long-term-induced cells did not vary among different substrates (data not shown). These experiments made a relevant contribution of integrins to the motile phenotype unlikely.

cDNA array analysis was then used to decipher whether the invasive phenotype conferred by BCL-x_L resulted from altered gene expression. Interestingly, these arrays linked the BCL-x_L effect to increased bioavailability of TGF-β_2 and MMPs (Figure 6). The loss of invasiveness of LNT-229 cells stably expressing small interfering TGF-$\beta_{1/2}$ RNA has been linked to the loss of MMP activity.[23] Appropriate control experiments using antibodies against TGF-β and a MMP inhibitor confirmed that the proinvasive effect of BCL-x_L entirely depended on these molecules (Figures 4a and 6b). These data do not differentiate between the necessity for TGF-β_2 in baseline and BCL-x_L-induced invasiveness. Further, the relative changes in TGF-β_2 expression within the LNT-229 BCL-x_L-inducible sublines are essential for the invasive phenotype not the apparent differences between these cells and controls at baseline. How overexpression of BCL-x_L for 21 but not for 3 days leads to a persistent induction of MMP-2, TGF-β_2 and membrane-bound MT1-MMP, remains to be elucidated. A direct transcriptional activity has not yet been ascribed to BCL-x_L and may be unlikely because of the prolonged time course. Alterations in integrin expression and activity have been excluded. MMP-2 and MT1-MMP were coinduced after expression of BCL-x_L for 21 days (Figure 6c and d). In contrast to squamous cell carcinomas, glioma cells exhibited no regulation of p mitogen-activated protein kinase (MAPK)/p extracellular-related kinase (ERK) (Table 1) to bridge the gap between survival pathways and regulation of MT1-MMP expression and hence invasiveness.[24] In contrast to the significant reduction of invasiveness, inhibiting TGF-β_2 or MMP-2 did not alter the sensitivity of control or BCL-x_L-inducible cells to CD95L/CHX-induced cell death, confirming two independent pathways to invasiveness or survival controlled by BCL-x_L (Figure 6e). Previously, BCL-x_L-induced downregulation of type 1 inositol 1,4,5-trisphosphate receptor had been linked to reduced T-cell antigen receptor ligation-induced Ca^{2+} flux in transgenic murine T cells and lower inositol 1,4,5-trisphosphate-mediated Ca^{2+} release capacity in microsomes.[25] This altered Ca^{2+} flux might influence the motility of glioma cells. However, in our cDNA arrays, we did not observe any relevant regulation of type 1 inositol 1,4,5-trisphosphate receptor (data not shown).

Importantly, overexpression of BCL-x_L also resulted in massive invasiveness of otherwise poorly invasive LNT-229 glioma cells *in vivo*. This occurred without an increase in the tumor volume, suggesting that the proinvasive effect of BCL-x_L is more relevant *in vivo* than the prosurvival effect. The invasive phenotype led to accelerated morbidity and mortality of the tumor-bearing mice. Further, the effect is sustained despite withdrawal from Dox *in vivo*. Interestingly, MMP inhibition displays a specific MMP-neutralizing effect both *in vitro* (Figure 4) and *in vivo* (Figure 7).

In summary, we delineate a novel pathway of BCL-x_L-induced invasiveness *in vitro* and demonstrate the induction of satellite formation of a noninvasive cell line in an intracranial xenograft model as a result of enhanced BCL-x_L expression. We illustrate the central roles of TGF-β_2 and MMP in these processes whereas altered sensitivity to *anoikis* or integrin expression or activity of MAPK/ERK were probably irrelevant for the newly characterized 'motility phenotype'.

Essentially, we have elucidated a novel consequence of long-term BCL-x_L overexpression independent from its antiapoptotic function, that is, conferring a delayed MMP-dependent invasive phenotype to malignant glioma cells which, in contrast to the resistance towards apoptosis, remains unaltered despite downregulation of BCL-x_L, establishing a unique paradigm for malignant glioma progression.

Materials and Methods

Reagents and cell culture

CHX, Dox, staurosporine and all other chemicals were purchased from Sigma (Deisenhofen, Germany) unless otherwise indicated. RO-28-2653 was kindly provided by Roche Diagnostics (Penzberg, Germany) and dissolved in DMSO at 15 μM for all *in vitro* applications. AnxV-FITC was purchased from BD PharMingen (Heidelberg, Germany). CD95L-containing supernatant (SN) was obtained from murine CD95L-transfected N2A murine neuroblastoma cells.[26] The human malignant glioma subline LN-229 was provided by Dr. N de Tribolet (Lausanne, Switzerland) but still harbors wild-type p53 and was therefore renamed LNT-229 (T for Tübingen) for clarification. NIH-3T3 murine fibroblasts were obtained from American Type Cell Culture (ATCC, Rockville, MD, USA). Cells were cultured in 75 cm^3 Falcon plastic flasks using Dulbecco's Modified Eagle's Medium (DMEM) supplemented with 2 mM glutamine (Life Technologies Inc., Paisley, UK), 10% fetal calf serum (FCS; Biochrom KG, Berlin, Germany) and penicillin (100 IU/ml)/streptomycin (100 μg/ml) and expanded by trypsin-EDTA (Life Technologies Inc.) treatment, and subcultured at a split ratio of 1 : 10 every 2–4 days. Cell cultures were routinely tested for contamination with *Mycoplasma* by 4′,6-diamidino-2-phenylindole staining. For acquisition of NIH-3T3-conditioned medium, the cells were grown in regular medium to subconfluent monolayers, washed with PBS, and incubated with serum-free DMEM for 48 h. SN was collected and stored at -20°C.

Generation of stable glioma cell sublines

Double-stably transfected LNT-229 BCL-x_L Tet-On glioma cell sublines were generated using the Tet-On Gene Expression System (Clontech, Palo Alto, CA, USA). Briefly, cDNA encoding the entire open reading frame of the human *bcl-x_L* gene was excised as a 0.8 kb *Eco*RI fragment from pBluescriptSK(+)-huBcl-x_L[27] and subcloned into pTRE to generate

pTRE-huBcl-x_L permitting conditional expression of BCL-x_L under the control of a TRE in the presence of Dox and of a rTetR. Restriction digest and sequence analysis verified correct cloning. To obtain a stable LNT-229 Tet-On glioma cell line, the cells were first transfected with the regulator plasmid pTet-On harboring cDNA encoding a rTetR fused in-frame to the transcriptional activation domain of the VP16 gene for expression of a reverse tetracycline-responsive transcriptional activator (rtTA) hybrid protein, and a *neomycin* resistance gene, using FuGENE (Roche, Basel, Switzerland) as a transfection reagent. Several G418-resistant stable cell clones were isolated by single-cell cloning and screened by transient transfections with the pTRE-Luc reporter plasmid and a standard luciferase reporter assay[28] for clones with low background expression and high Dox-dependent (2 μg/ml) inducing of the rtTA regulatory protein. Selected stably transfected LNT-229 Tet-On glioma cell clones (designated c4.2, c10.1, and c34.2) served as nonBCL-x_L-inducible control cells in all experiments. In a second selection step, the pTRE-huBcl-x_L response plasmid was introduced into these clones by cotransfection with pTK-Hyg harboring a *hygromycin* resistance gene to allow selection of stably transformed cells in the presence of hygromycin. Several G418- and hygromycin-resistant cell clones were isolated by single cell cloning and screened by immunoblot analysis for clones with low background expression and high Dox-dependent (2 μg/ml) inducing of BCL-x_L protein. These clones (designated c4.2E, c10.1D, c10.1J and c34.2A) were included in the experiments and gave similar results. Representative data are shown for c10.1/c10.1D, c10.1/c10.1J and c34.2/c34.2A.

Immunoblot

SN generated in the absence of FCS were concentrated using the Centriplus centrifugal filter device YM-3 (3.0 kDa cut-off; Millipore, Eschborn, Germany). Cell lysates were prepared in 50 mM Tris-HCl (pH 8.0) containing 120 mM NaCl, 5 mM EDTA, 0.5% Nonidet P-40, 2 μg/ml aprotinin, 10 μg/ml leupeptin and 100 μg/ml phenylmethylsulfonyl fluoride. Aliquots of concentrated SN or cell lysates were electrophoresed on 8-12% SDS-PAGE gels under reducing conditions and transferred to nitrocellulose (Schleicher & Schuell, Dassel, Germany). The lysates and SN were assessed at 20 μg of total protein per lane. Equal protein loading was ascertained by Ponceau S staining. After blocking nonspecific-binding sites with 5% (w/v) dried milk in PBS for 30 min, the filters were incubated with specific primary antibodies overnight at 4°C, washed and incubated with horseradish peroxidase-conjugated donkey anti-goat IgG, goat anti-mouse IgG or goat anti-rabbit IgG (diluted 1 : 3000) (Santa Cruz Biotechnology, Santa Cruz, CA, USA) for 3 h at 22°C. The primary antibodies sc-1616 goat anti-β-actin (Santa Cruz Biotechnology), 2H12 mouse anti-BCL-x (BD Biosciences, Heidelberg, Germany), sc-94 rabbit anti-MAPK/ERK1 (Santa Cruz Biotechnology), E10 mouse anti-Phospho-p44/42-MAPK (Cell Signaling Technology, Beverly, MA, USA), Ab-3 mouse anti-MMP-2 (Oncogene, San Diego, CA, USA), Ab-7 mouse anti-MMP-9 (Oncogene, San Diego, CA, USA), Ab-4 mouse anti-MT1-MMP (Oncogene), sc-8008 mouse anti-NFκB (Santa Cruz Biotechnology), sc-146 rabbit anti-TGF-β_1 (Santa Cruz Biotechnology), sc-90 rabbit anti-TGF-β_2 (Santa Cruz Biotechnology) or M56L mouse anti-TIMP-2 (Oncogene) were used at 1 μg/ml (anti-β-actin, anti-BCL-x), 2 μg/ml (anti-MMP-9, anti-TGFβ_2, anti-TIMP-2) or 5 μg/ml (anti-MT1-MMP) in PBS containing 0.05% Tween 20 and 5% skim milk. Furin antiserum was used as described previously.[29] Protein bands were visualized using enhanced chemiluminescence (Amersham, Braunschweig, Germany) and quantified by multiplying the respective signal area of each protein band with its mean intensity using Corel Photo Paint 11 software (Corel Cooperation, Ottawa, Canada) and normalizing to the values of untreated inducible and control samples.

RT-PCR

Total RNA was isolated using the RNeasy kit, cDNA was generated and amplification for MMP-2 was carried out using standard protocols The condition for all polymerase chain reactions were 40 cycles of 95°C for 15 s and 60°C for 1 min. Data analysis was carried out by using the ΔC_T method for relative quantification. Briefly, threshold cycles (C_T values) for 18S rRNA (reference) and MMP-2 (sample) were determined in duplicates. We arbitrarily defined the values obtained for control cells as the standard value (100%) and determined the relative change (*rl*) in copy numbers according to the formula $rl = 2-[(C_{T\ \text{Sample}}-C_{T\ \text{Reference}})-(C_{T\text{Standard sample}}-C_{T\text{Standard reference}})]$.[30]

Immunofluorescence

The cells were seeded into 24-well plates containing poly-L-lysine-coated coverslips and allowed to attach for 24 h in complete medium with or without Dox (2 μg/ml). The medium was replaced with fresh medium containing 100 nM MitoTracker Red CMXRos (Molecular Probes Europe, Leiden, The Netherlands), a red-fluorescent dye that accumulates in mitochondria of live cells depending on the mitochondrial membrane potential. After 30 min the cells were washed with PBS, fixed in 4% paraformaldehyde for 15 min, treated three times with PBS-containing 0.1% bovine serum albumine and 0.1% saponine and incubated at 4°C overnight with polyclonal rabbit anti-BCL-x antibody (BD Biosciences) or with control antibody (PBS/0.1% BSA/0.1% saponine) only. Following three washing steps, the cells were stained light-safe with a FITC-conjugated Alexa Fluor 488 goat anti-rabbit secondary antibody (1 : 50; Molecular Probes) for 3 h at room temperature, washed three times and mounted in Mowiol 4–88 mounting medium (Calbiochem, Schwalbach, Germany) for confocal analysis in dual channels using a Zeiss Axiovert 100 M confocal laser-scanning microscope and LSM 510 software (Zeiss, Göttingen, Germany).

Gelatin zymography

MMP-2/-9 activity was analyzed as described.[12] Briefly, 20 μg of soluble SN protein was separated by 10% SDS-PAGE containing 0.1% gelatin (wt/vol) without denaturing agents (Bio-Rad, Munich, Germany). These were washed twice for 30 min in 50 mM Tris-HCl, pH 7.5 and 2.5% Triton X-100 and incubated overnight at 37°C in 50 mM Tris-HCl, pH 7.6, 10 mM $CaCl_2$, 150 mM NaCl, and 0.05% NaN_3 with or without RO-28-2653 (15 μM). Coomassie Brillant Blue R-250 staining and subsequent destaining with 90% methanol/H_2O (1:1) and 10% glacial acetic acid resulted in decreased staining at the level of electrophoretic migration of MMP-2 (72 kDa). *In situ* zymography was performed by incubating cryostat transverse mouse brain sections (8 μm) with 40 μg/ml Oregon Green 488 conjugated gelatin (Molecular Probes) in 50 mM Tris-HCl, pH 7.4, 7.5 mM $CaCl_2$, 150 mM NaCl, and 0.05% Brij-35 (Calbiochem) overnight at 37°C. Gelatinolytic proteases cleave quenched fluorescence-conjugated gelatin resulting in fluorescent breakdown products that thereby allow for the localization of net gelatinolytic activity. Addition of 10 mmol/l ethylenediaminetetraacetic acid (EDTA), a chelating agent that inhibits metal ion-dependent proteases such as MMPs, to the assay solution or omission of the substrate served as negative controls. Sections were washed three times with PBS and mounted with DAPI-containing Vectashield (Vector Laboratories, Burlingame, CA, USA).[30] Green fluorescent gelatinase activity and DAPI fluorescence were visualized in dual channels using a Zeiss Axioplan 2 fluorescence microscope (Zeiss, Jena, Germany) and each image was processed at identical settings using Zeiss AxioVision 4.3 software.

cDNA array analysis

Total RNA was isolated using the RNeasy Mini Kit (Qiagen, Hilden, Germany). The Atlas Human Cancer 1.2 and Apoptosis Arrays (Clontech) were used to screen for alterations of gene expression by Dox treatment in c10.1 or c10.1J cells. Details for cDNA probe synthesis, array hybridization, and quantification have been described.[31] A Dox-treated to control ratio of ≥ 1.5 in expression was considered as a relevant upregulation whereas a ratio of < 0.67 in expression was considered as a downregulation.

Flow cytometry and apoptosis assays

Staurosporine-induced apoptosis was examined by AnxV-FITC staining. The cells were grown in six-well plates, incubated with staurosporine (20 μM) for 6 h, washed in PBS and resuspended in 10 mM HEPES/NaOH, pH 7.4, 140 mM NaCl and 2.5 $CaCl_2$. AnxV-FITC (1 : 100) and PI (50 μg/ml) were added and fluorescence in a total of 10 000 events per condition was recorded in a FACScalibur (Becton Dickinson, Heidelberg, Germany). AnxV-FITC- or PI-positive cells were counted as dead cells (either apoptotic or necrotic) and the remaining cells were designated the surviving cell fraction. Viable cell density following 12 h of incubation with CD95L (120 U/l) and CHX (10 μg/ml) was assessed by crystal violet staining.[10]

Clonogenicity and proliferation assays

Clonogenicity was assayed by suspending glioma cells at a dilution of 500 cells/ml in complete medium with or without Dox (2 μg/ml) per well in six-well plates and counting the number of macroscopically visible clones (> 0.15 mm in diameter) after 10–14 days. To assess proliferation, the cells were seeded in 96-well plates (1500 cells/well) in triplicates and cultured in complete medium with or without Dox (2 μg/ml). The cells were pulsed with [methyl-^{3}H]-thymidine (1 μCi; Amersham) on day 3 and collected 16 h later using a cell harvester (Tomtec, Hamden, CT, USA). Incorporated radioactivity was determined in a Wallac 1450 Microbeta Plus Liquid Scintillation Counter (Wallac, Turku, Finland).

Glucose assay

For the assessment of glucose metabolism, glucose concentrations in the SN of glioma cells were determined by the hexokinase/G6P-DH method employing the Gluco-quant Glucose/HK kit (Roche).

ATP assay

Plates were placed on ice, and the cells were pelleted by centrifugation and lysed in ATP-releasing agent (Sigma). ATP was determined by luciferase assay with the CLS II kit (Boehringer, Mannheim, Germany).[32]

Matrigel invasion assay

Invasion of glioma cells *in vitro* was measured in Boyden chamber assays (BD Biosciences). Briefly, pretreated subconfluent glioma cells were harvested in enzyme-free cell dissociation buffer (Gibco Life Technologies, Karlsruhe, Germany) and diluted in complete medium with or without Dox (2 μg/ml), *o*-PA (5 μM), RO-28-2653 (15 μM) and DMSO, zVAD-fmk (10 μM; Biomol, Hamburg, Germany) or neutralizing TGF-β_2 or isotype control antibodies (2 μg/ml; Sigma). The cell suspension (2×10^5 cells/ml, 200 μl) per condition was added in triplicates to each matrigel-coated transwell insert. NIH 3T3-conditioned medium (500 μl) was used as a chemoattractant in the lower wells. Following an incubation period of 20 h, the cells on the lower side of each membrane were fixed in methanol at 4°C, stained with toluidine blue and sealed on slides. Photographs of representative microscopical fields were taken at 100-fold magnification. Quantification of cell invasion was expressed as the mean count of stained cells in five random fields of each membrane.

Spheroid invasion assay

Multicellular glioma spheroids were obtained by seeding glioma cells (3×10^4 cells/ml) in 96-well plates that were base coated with 1.0% Noble Agar (Difco Laboratories, Detroit, MI, USA) prepared in DMEM and culturing for 4–5 days until spheroids had formed. The extracellular matrix gel was prepared by mixing collagen I solution (Vitrogen 100, Cohesion, Palo Alto, CA, USA) and minimal essential medium at a 8 : 1 ratio at 4°C with or without Dox (2 μg/ml), RO-28-2653 (15 μM) or its vehicle DMSO, supplementing human fibronectin (10 μg/ml) and adjusting the pH by addition of NaOH/$NaHCO_3$. This solution (400 μl) was added into 12-well plates and spheroids of defined size (~ 250 μm) were implanted into the gel in triplicates. After gelation at 37°C, the gel was overlaid with 400 μl of complete medium and cultured in a humidified atmosphere (37°C; 5% CO_2). The spreading of the spheroids was monitored by microscopic photographs of each spheroid after 0, 24, 48 and 72 h. For quantification, the mean radial distance of 30 randomly selected glioma cells that had migrated from the tumor spheroid into the gel matrix was measured in intervals of 24 h, and expressed in relation to the mean radial distance at time 0 h.

Animal studies and immunohistochemistry

All animal work was performed in accordance with the NIH guidelines *Guide for the Care and Use of Laboratory Animals*. In all 10^5 human c34.2A or c34.2 glioma cells that had not been pretreated with Dox *in vitro* were suspended in 4 μl PBS and implanted stereotactically into the right striatum of 6–12 weeks old athymic mice (CD1 *nu/nu*; Charles River, Sulzfeld, Germany).[33] Three independent groups of animals (each $n = 9$) were formed: Dox (2 mg/ml) dissolved in a 1% sucrose solution was applied as drinking water of mice that had been implanted c34.2 control cells (group 1) or of c34.2A-bearing mice (group 2). As a further control group, mice bearing c34.2A cells received sucrose solution only (group 3). For the assessment of tumor growth, mice ($n = 2$) of each group were killed on day 28 after tumor cell implantation. Cryostat transverse brain sections (8 μm) were stained with hematoxylin–eosin. For the immunohistochemical detection of BCL-x_L, cryostat brain sections were treated with 3% H_2O_2 (15 min) for inactivation of endogenous peroxidases, subsequently incubated in citrate buffer (pH 6.0) at 95°C for 20 min, blocked in Roti-Block (Roth, Karlsruhe, Germany) (1 : 10) for 15 min and in 10% goat serum (Tris-HCl, pH 8.0, as diluent) for 10 min and incubated overnight at 4°C with a rabbit polyclonal anti-human BCL-x antibody (Dako, Carpinteria, CA, USA) (1 : 50, Tris-HCl as diluent) or an unspecific rabbit IgG antibody as isotype control (Vector Laboratories) (1 : 1500). Expression of BCL-x_L was detected using a biotinylated goat anti-rabbit secondary antibody (Vector Laboratories) (1 : 200; 45 min) and the Vectastain Elite avidin–biotin complex kit (Vector Laboratories) with nickel-intensified 3,3′-diaminobenzidine (DAB) as chromagen. For survival analyses, animals of each group ($n = 7$) were observed by a blinded investigator in daily intervals and killed by an overdose of anesthetic at the onset of neurological symptoms. For assessing both the *in vivo* effects of

the MMP-2/-9-specific inhibitor RO-28-2653 and the effects of *in vivo* downregulation of BCL-x_L preceded by an initial long-term induction of its expression *in vitro*, c34.2A glioma cells were pretreated with Dox 2 μg/ml *in vitro* for 21 days and were subsequently implanted intracerebrally as described above. Three groups of animals were formed: Dox application (2 mg/ml) was continued *via* the drinking water in the absence (group 1; $n=4$) or presence of RO-28-2653 (group 2; $n=6$) that was applied by oral gavage (100 mg/kg) twice daily from day 8–28 after implantation. Dox application was discontinued *in vivo* by applying sucrose solution only (group 3; $n=4$). To guarantee equal experimental conditions in each animal group, mice of group 1 and 3 received two daily oral gavages of the polymer vehicle substance of Eudragit (100 mg/kg; Roche). For the assessment of tumor growth, all animals were killed on day 28 after tumor cell implantation. Cryostat transverse brain sections (8 μm) were stained with hematoxylin–eosin, and tumor-containing sections of each brain were used for *in situ* zymographies. Glioma satellite formation was quantified at arbitrary units by a blinded investigator.[34]

Statistical analysis

Quantitative data obtained for flow cytometry, number of crystal violet-positive cells, Boyden chamber invasion and spheroid invasion are expressed as mean and S.E.M., as indicated. Statistical significance was assessed by one way ANOVA followed by Tukey's *post hoc* test. All *in vitro* experiments reported here represent at least three independent replications performed in triplicate. *P*-values for the protein expression profile and for the formation of tumor satellites from xenografted gliomas were derived from two-tailed Student's *t*-tests. Values of $P<0.05$ were considered significant, and $P<0.01$ were considered highly significant (Excel, Microsoft, Seattle, WA, USA). Evaluation of survival patterns in mice bearing intracerebral gliomas was performed by the Kaplan–Meier method.[35]

Acknowledgements

We thank Yasmin Breithardt, Brigitte Frank, Gabriele von Kürthy and Ulrike Obermüller for excellent technical assistance. This work was supported by grant WI-1835/1-1 from the German National Research Foundation to WW.

References

1. Bögler O and Weller M (2003) International Hermelin Brain Tumor Center Symposium on apoptosis. Cell Death Differ. 10: 1112–1115
2. Plas DR, Talapatra S, Edinger AL, Rathmell JC and Thompson CB (2001) Akt and BCL-x_L promote growth factor-independent survival through distinct effects on mitochondrial physiology. J. Biol. Chem. 276: 12041–12048
3. Jeong S-Y, Gaume B, Lee Y-J, Hsu Y-T, Ryu S-W, Yoon S-H and Youle RJ (2004) BCL-x_L sequesters its C-terminal membrane anchor in soluble, cytosolic homodimers. EMBO J. 23: 2146–2155
4. Kaufmann T, Schlipf S, Sanz J, Neubert K, Stein R and Borner C (2002) Characterization of the signal that directs BCL-x_L, but not BCL-2, to the mitochondrial outer membrane. J. Cell Biol. 160: 53–64
5. Bourguignon LY, Zhu H, Shao L and Chen YW (2000) CD44 interaction with c-Src kinase promotes contraction-mediated cytoskeleton function and hyaluronic acid (HA)-dependent ovarian tumor cell migration. J. Biol. Chem. 276: 7327–7336
6. Hiscox S and Jiang WG (1997) Regulation of endothelial CD44 expression and endothelium-tumour cell interactions by hepatocyte growth factor/scatter factor. Biochem. Biophys. Res. Commun. 233: 1–5
7. Lund-Johansen M, Bjerkvig R, Humphrey PA, Bigner SH, Bigner DD and Laerum OD (1990) Effect of epidermal growth factor on glioma cell growth, migration, and invasion *in vitro*. Cancer Res. 50: 6039–6044
8. Laterra J, Nam M, Rosen E, Rao JS, Lamszus K, Goldberg ID and Johnston P (1997) Scatter factor/hepatocyte growth factor gene transfer enhances glioma growth and angiogenesis *in vivo*. Lab. Invest. 76: 565–577
9. Merzak A, McCrea S, Koocheckpour S and Pilkington GJ (1994) Control of human glioma cell growth, migration, and invasion *in vitro* by transforming growth factor beta 1. Br. J. Cancer 70: 199–203
10. Wick W, Grimmel C, Wild-Bode C, Platten M, Arpin M and Weller M (2001) Ezrin-dependent promotion of glioma cell clonogenicity, motility and invasion mediated by BCL-2 and TGF-β_2. J. Neurosci. 21: 3360–3368
11. Uhl M, Aulwurm S, Wischhusen J, Weiler M, Almirez R, Mangadu R, Liu YW, Platten M, Herrlinger U, Murphy A, Wick W, Higgins L and Weller M (2004) SD-208, a novel TGF-β receptor I antagonist, inhibits growth and invasiveness and enhances immunogenicity of murine and human glioma cells *in vitro* and *in vivo*. Cancer Res. 64: 7954–7961
12. Wick W, Wagner S, Kerkau S, Dichgans J, Tonn JC and Weller M (1998) BCL-2 promotes migration and invasiveness of human glioma cells. FEBS Lett. 440: 419–424
13. Uhm J, Dooley N, Kyritsis A, Rao J and Gladson C (1999) Vitronectin, a glioma-derived extracellular matrix protein, protects tumor cells from apoptotic death. Clin. Cancer Res. 5: 1587–1594
14. Nör J, Christensen J, Liu J, Peters M, Mooney DJ, Strieter RM and Polverini PJ (2001) Up-regulation of BCL-2 in microvascular endothelial cells enhances intratumoral angiogenesis and accelerates tumor growth. Cancer Res. 61: 2183–2188
15. Wild-Bode C, Weller M and Wick W (2001) Molecular determinants of glioma cell migration and invasion. J. Neurosurg. 94: 978–984
16. Ruoslahti E and Reed J (1999) New way to activate caspases. Nature 397: 479–480
17. Roelle S, Grosse R, Aigner A, Krell HW, Czubayko F and Gudermann T (2003) Matrix metalloproteinase 2 and 9 mediate epidermal growth factor receptor transactivation by gonadotropin-releasing hormone. J. Biol. Chem. 278: 47307–47318
18. Wang H-G, Rapp UR and Reed JC (1996) Bcl-2 targets the protein kinase Raf-1 to mitochondria. Cell 87: 629–638
19. Kroemer G (1997) The proto-oncogene BCL-2 and its role in regulating apoptosis. Nat. Med. 3: 614–620
20. Gross A, Yin XM, Wang K, Wei MC, Jockel J, Milliman C, Erdjument-Bromage H, Tempst P and Korsmeyer SJ (1999) Caspase cleaved BID targets mitochondria and is required for cytochrome c release, while BCL-X_L prevents this release but not tumor necrosis factor-R1/Fas death. J. Biol. Chem. 274: 1156–1163
21. Frisch SM and Francis H (1994) Disruption of epithelial cell–matrix interactions induces apoptosis. J. Cell Biol. 124: 619–626
22. Buckley CD, Pilling D, Henriquez NV, Parsonage G, Threlfall K, Scheel-Toellner D, Simmons D-L, Akbar AN, Lord JM and Salmon M (1999) RGD peptides induce apoptosis by direct caspase-3 activation. Nature 397: 534–539
23. Friese MA, Wischhusen J, Wick W, Weiler M, Eisele G, Steinle A and Weller M (2004) RNA interference targeting transforming growth factor-beta enhances NKG2D-mediated antiglioma immune response and inhibits glioma cell migration and invasiveness, and abrogates tumorigenicity *in vivo*. Cancer Res. 64: 7596–7603
24. Munshi HG, Wu YI, Mukhopadhyay S, Ottaviano AJ, Sassano A, Koblinski JE, Platanias LC and Stack MS (2004) Differential regulation of membrane type 1-matrix metalloproteinase activity by ERK1/2- and p38 MAPK-modulated tissue inhibitor of metalloproteinase 2-expression controls transforming growth factor-beta1-induced pericellular collagenolysis. J. Biol. Chem. 279: 39042–39050
25. Li C, Fox CJ, Master SR, Bindokas VP, Chodosh LA and Thompson CB (2002) BCL-X(L) affects Ca(2+) homeostasis by altering expression of inositol 1,4,5-trisphosphate receptors. Proc. Natl. Acad. Sci. USA 99: 9830–9835
26. Rensing-Ehl A, Frei K, Flury R, Matiba B, Mariani SM, Weller M, Aebischer P, Krammer PH and Fontana A (1995) Local Fas/APO-1 (CD95) ligand-mediated tumor killing *in vivo*. Eur. J. Immunol. 25: 2253–2258
27. Boise LH, Gonzalez-Garcia M, Postema CE, Ding L, Lindsten T, Turka LA, Mao X, Nunez G and Thompson CB (1993) Bcl-x, a bcl-2-related gene that functions as a dominant regulator of apoptotic cell death. Cell 74: 597–608

28. Wischhusen J, Naumann U, Ohgaki H, Rastinejad F and Weller M (2003) CP-31398, a novel p53-stabilizing agent, induces p53-dependent and p53-independent glioma cell death. Oncogene 22: 8233–8245
29. Leitlein J, Aulwurm S, Waltereit R, Naumann U, Wagenknecht B, Garten W, Weller M and Platten M (2001) Processing of immunosuppressive pro-TGF-$\beta_{1/2}$ by human glioblastoma cells involves cytoplasmic and secreted furin-like proteases. J. Immunol. 166: 7238–724330
30. Lambert V, Wielockx B, Munaut C, Galopin C, Jost M, Itoh T, Werb Z, Baker A, Libert C, Krell HW, Foidart JM, Noel A and Rakic JM (2003) MMP-2 and MMP-9 synergize in promoting choroidal neovascularization. FASEB J. 17: 2290–2292
31. Huang H, Colella S, Kurrer M, Yonekawa Y, Kleihues P and Ohgaki H (2000) Gene expression profiling of low-grade diffuse astrocytomas by cDNA arrays. Cancer Res. 60: 6868–6874
32. Steinbach JP, Wolburg H, Klumpp A, Probst H and Weller M (2003) Hypoxia-induced cell death in human malignant glioma cells: energy deprivation promotes decoupling of mitochondrial cytochrome c release from caspase processing and necrotic cell death. Cell Death Differ. 10: 823–832
33. Fulda S, Wick W, Weller M and Debatin KM (2002) Smac agonists sensitize for Apo2L/TRAIL- or anticancer drug-induced apoptosis and induce regression of malignant glioma *in vivo*. Nat. Med. 8: 808–815
34. Wild-Bode C, Weller M, Rimner A, Dichgans J and Wick W (2001) Sublethal irradiation promotes migration and invasiveness of glioma cells: implications for radiotherapy of human glioblastoma. Cancer Res. 61: 2744–2750
35. Kaplan EL and Meyer P (1958) Non-parametric estimation from incomplete observations. J. Am. Stat. Assoc. 53: 457–481